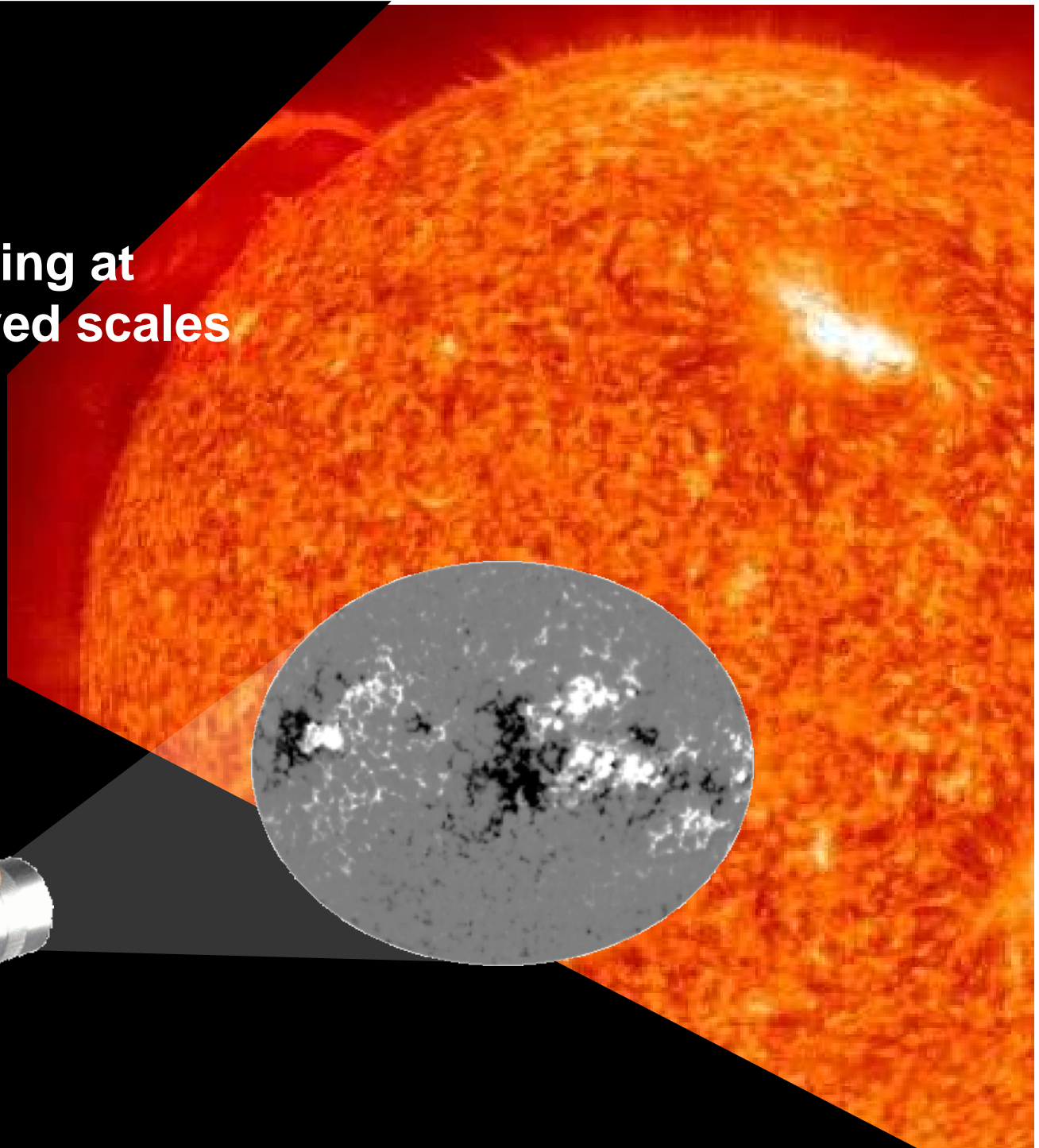
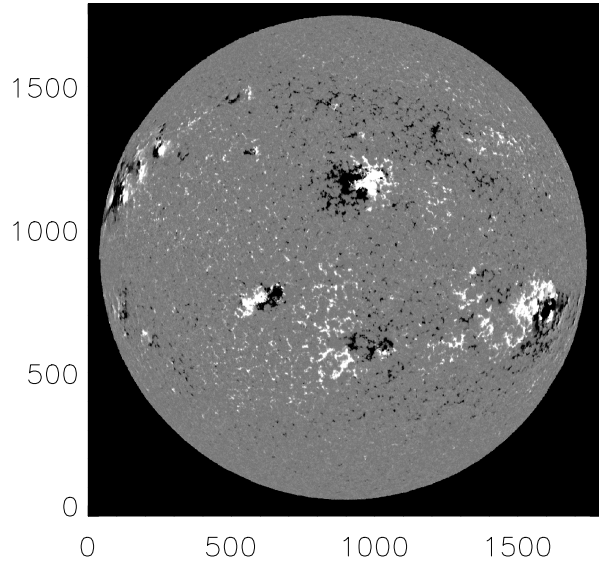


# Magnetic structuring at spatially unresolved scales

**Jan Stenflo**  
*ETH Zurich and  
IRSOL, Locarno*



18 Mar 2000

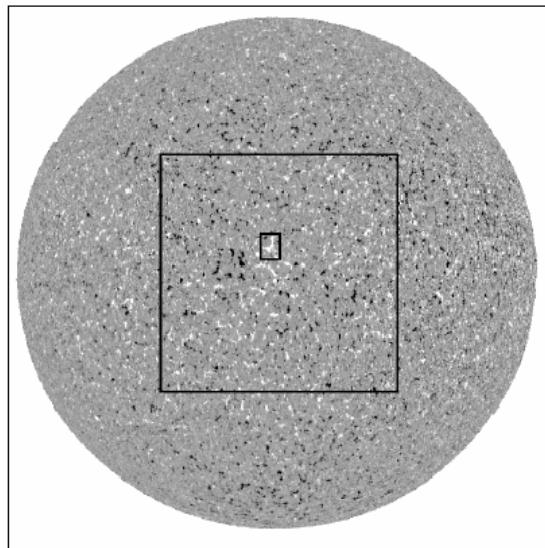
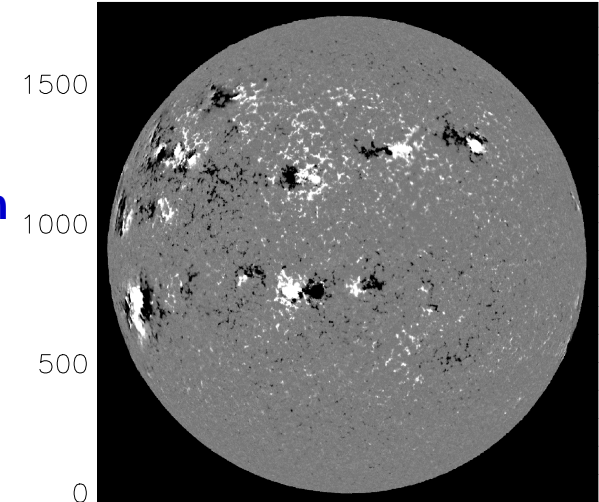


## Magnetograms of the active and quiet Sun

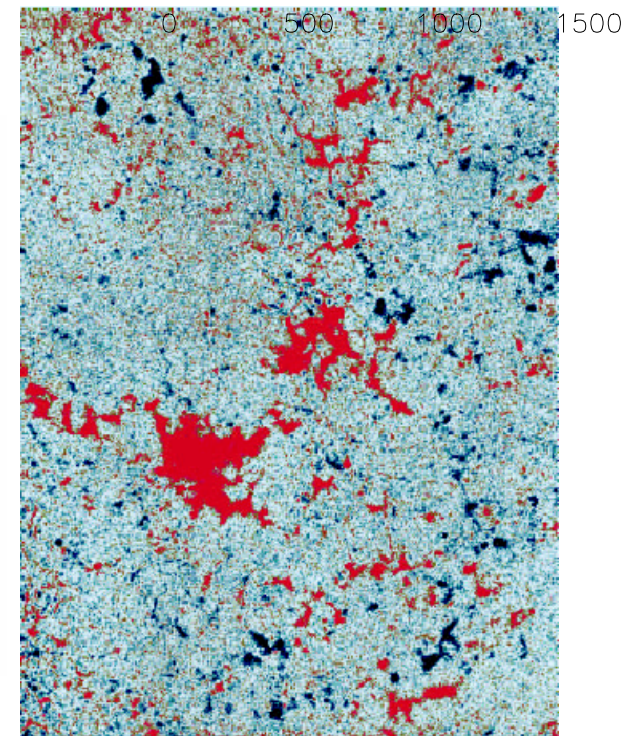
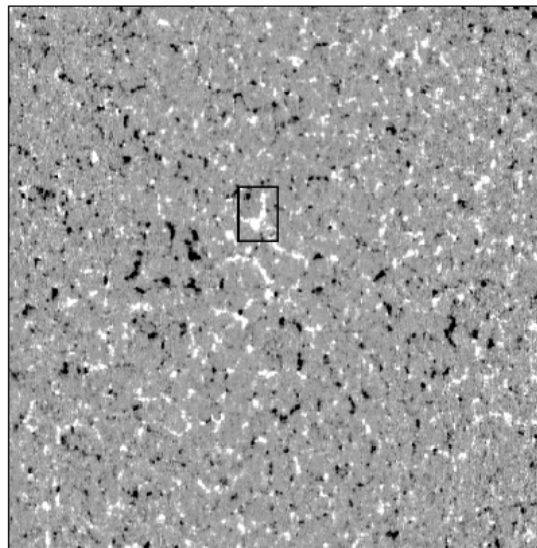
**Question: What would the field look like with infinite resolution**

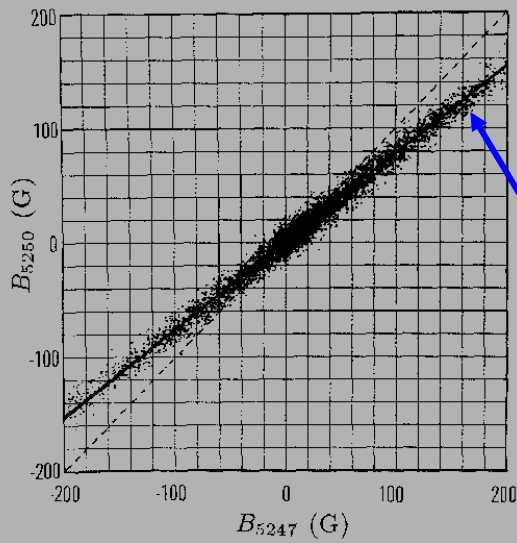
**To answer this question the line-ratio technique was introduced in 1971**

26 Feb 2000



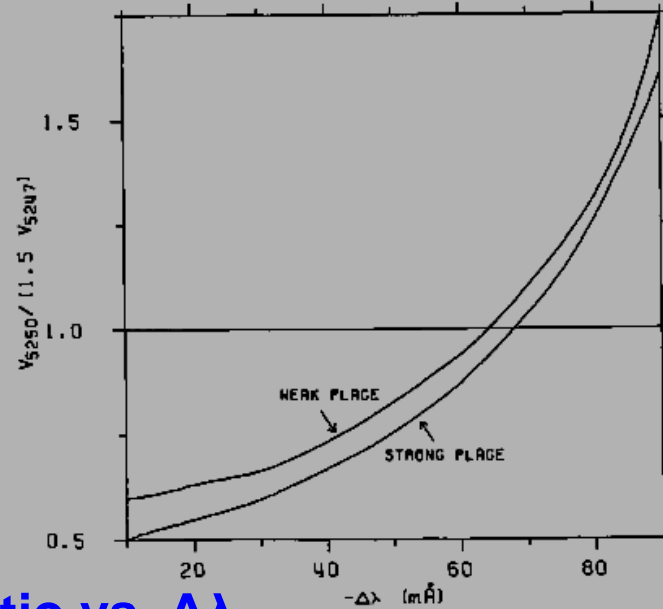
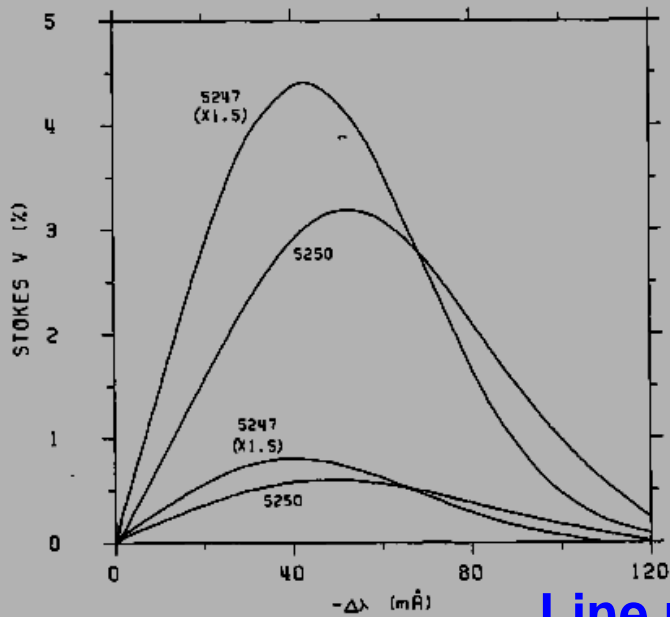
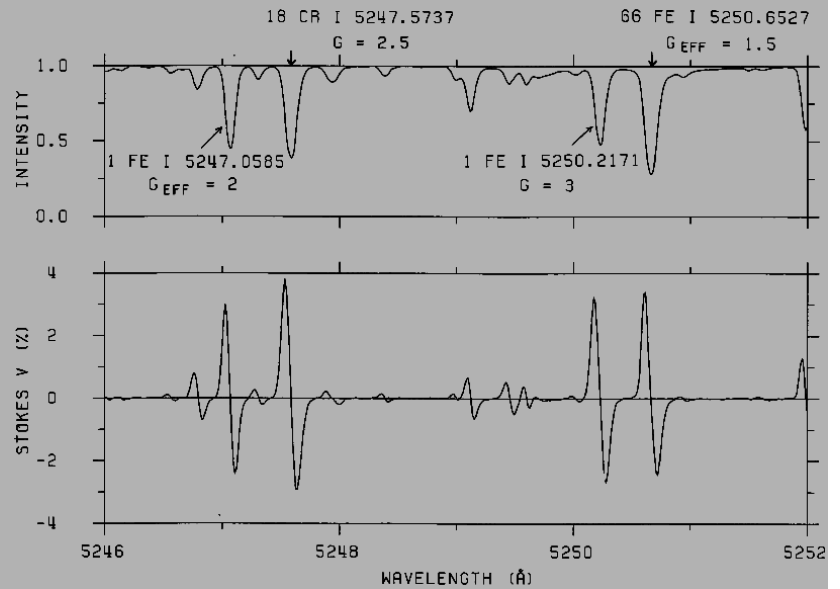
9 February 1996





## 5250 / 5247 line ratio technique

Slope gives intrinsic field strength

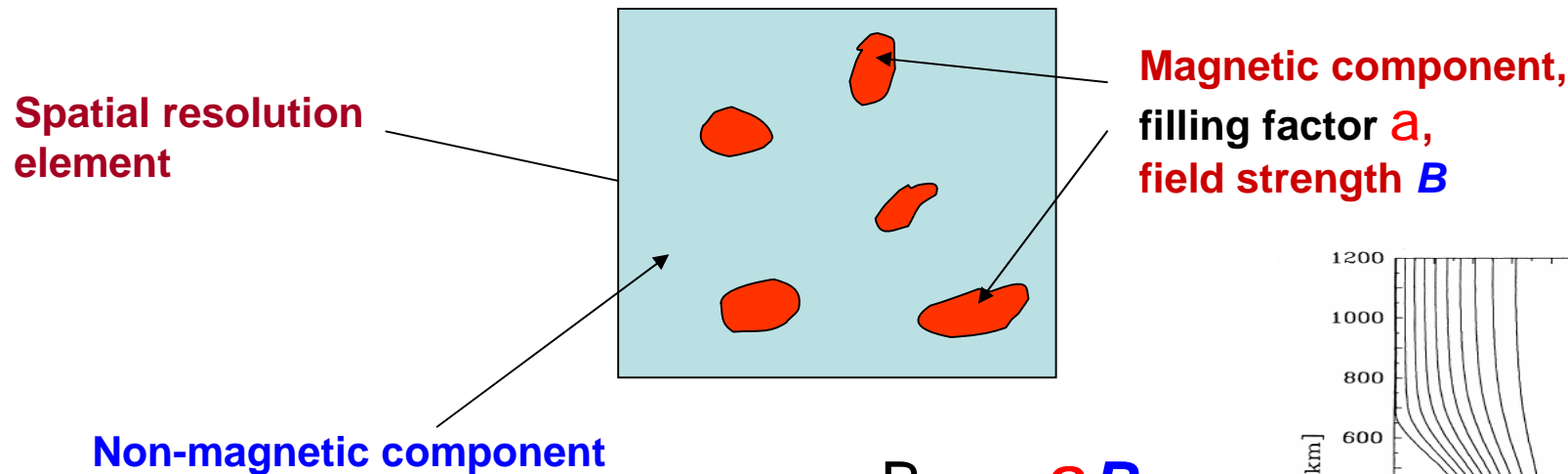


## Line ratio vs. $\Delta\lambda$

(verifies physical validity of the model)

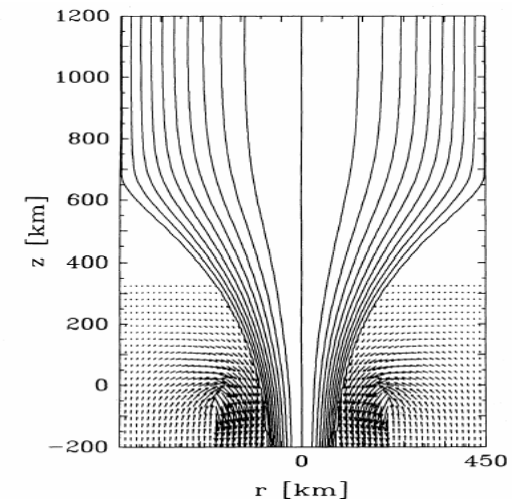


# For the interpretation of the line-ratio data a **2-component** model was introduced



$$\langle B \rangle = aB$$

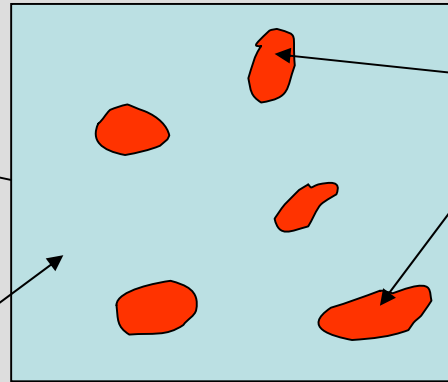
Since with the two-component model  $B$  is found to be 1 - 2 kG, while  $a$  is typically about 1%, the concept of intermittent **magnetic flux tubes** was introduced



**The flux tubes became the theoretical counterpart of the 2-component model**

# Extension of the 2-component model through use of the Hanle effect

Spatial resolution element

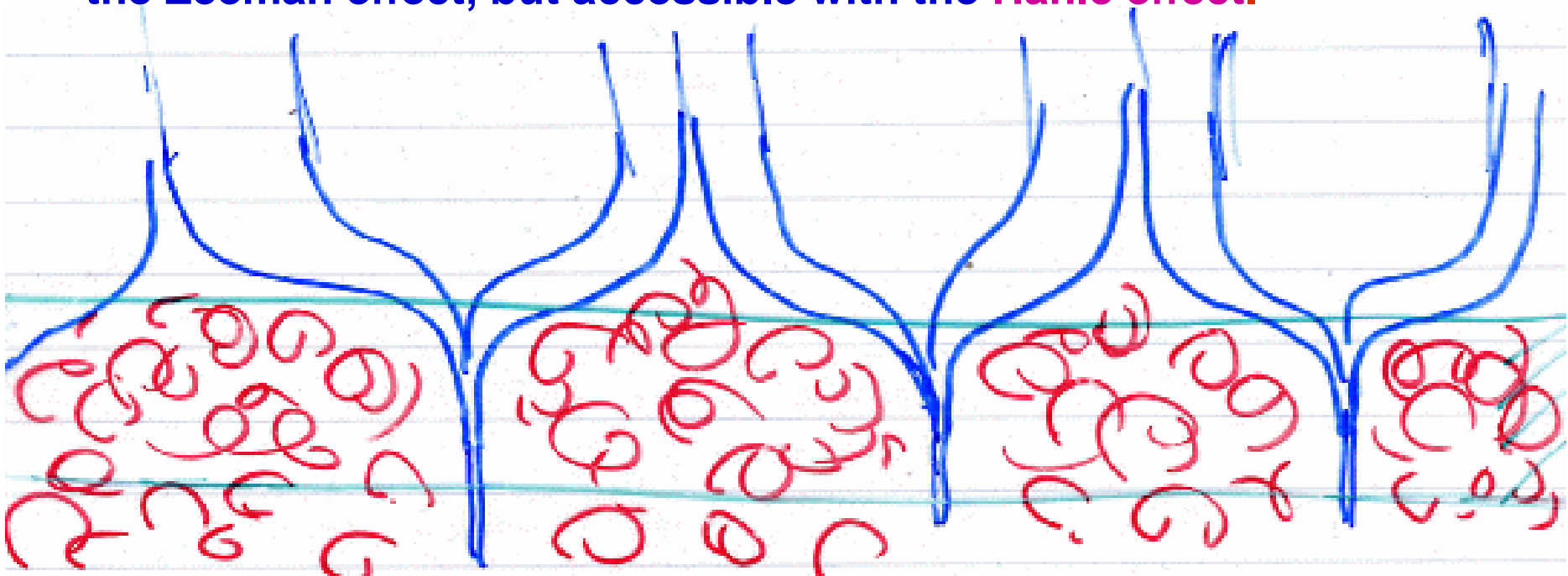


Magnetic component,  
filling factor  $a$ ,  
field strength  $B$

Not a “non-magnetic” atmosphere  
but a mixed-polarity, tangled  
or turbulent field

## Resulting “standard model”

- **Flux tubes** expanding with height, forming canopies above the photosphere. Contribute to the **Zeeman effect**.
- **Weaker tangled or turbulent field** in between. No information from the Zeeman effect, but accessible with the **Hanle effect**.



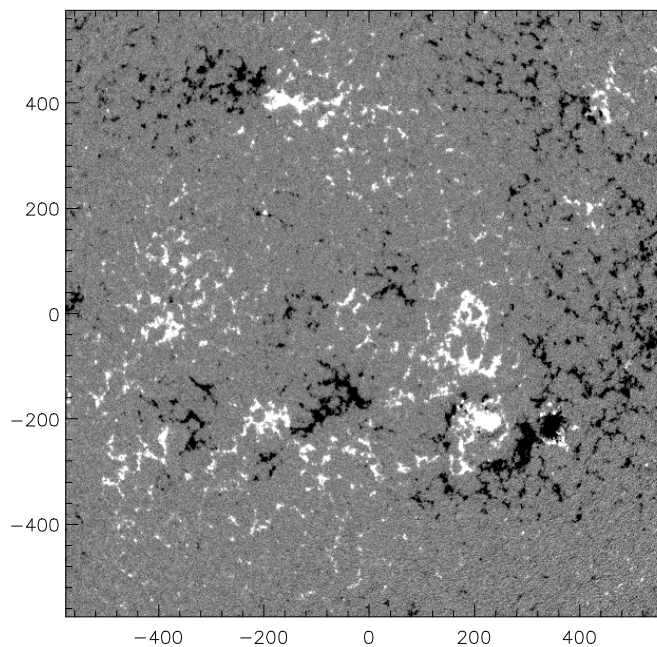
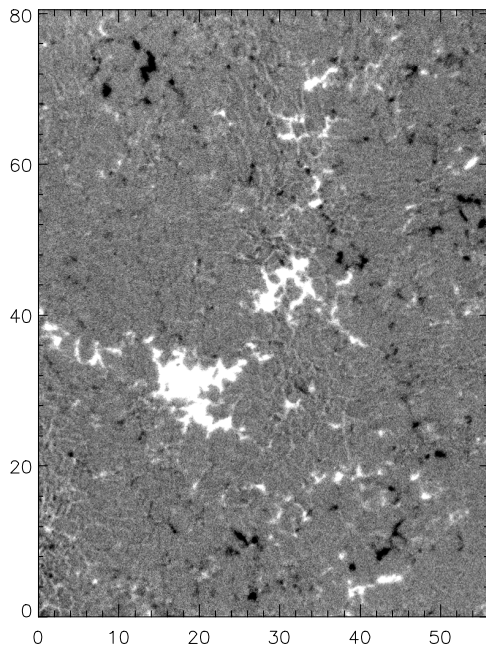
This **dualistic scenario** is however an artefact of applying two diagnostic tools, which are highly complementary: the Zeeman and Hanle effects.

**The real world is not dualistic.**

**La Palma magnetogram  
9 February 1996**

**MDI magnetogram  
20 March 2002**

The area of the left magnetogram is only 0.35 % of the area covered by the right one (scale in arcsec)

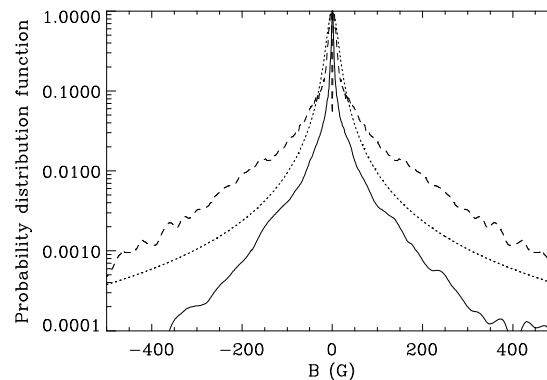
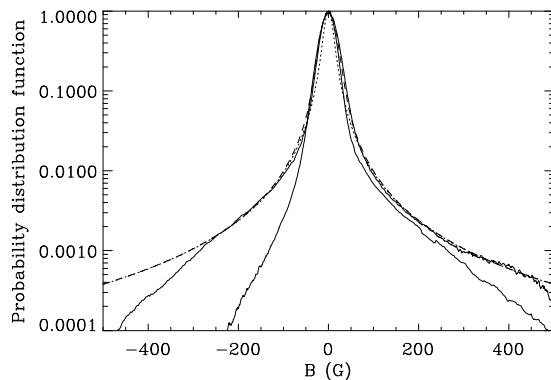


**Fractal patterns  
of observed  
flux densities.**

**Scale invariance**

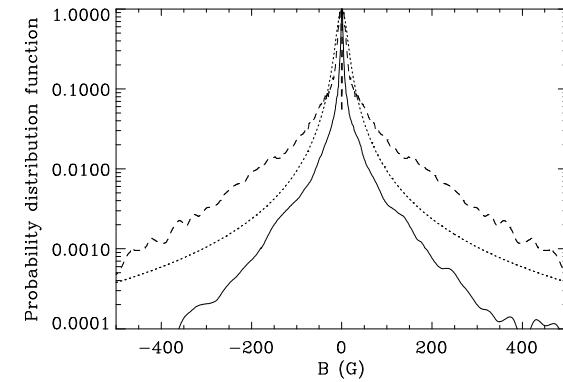
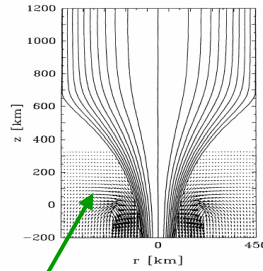
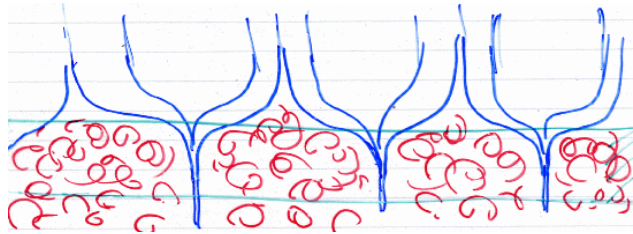
**Empirical PDFs:  
La Palma (thick), MDI (thin),  
Voigt profile (dashed)**

**Comparison between theory (Stein & Nordlund 2002;  
solid line for  $B_z$ , dashed line for  $|B|$ )  
and the empirical Voigt function (dotted)**



**Probability distribution  
functions PDF**

**From Stenflo & Holzreuter 2002**



$\delta$  function peak for "non-magnetic" component

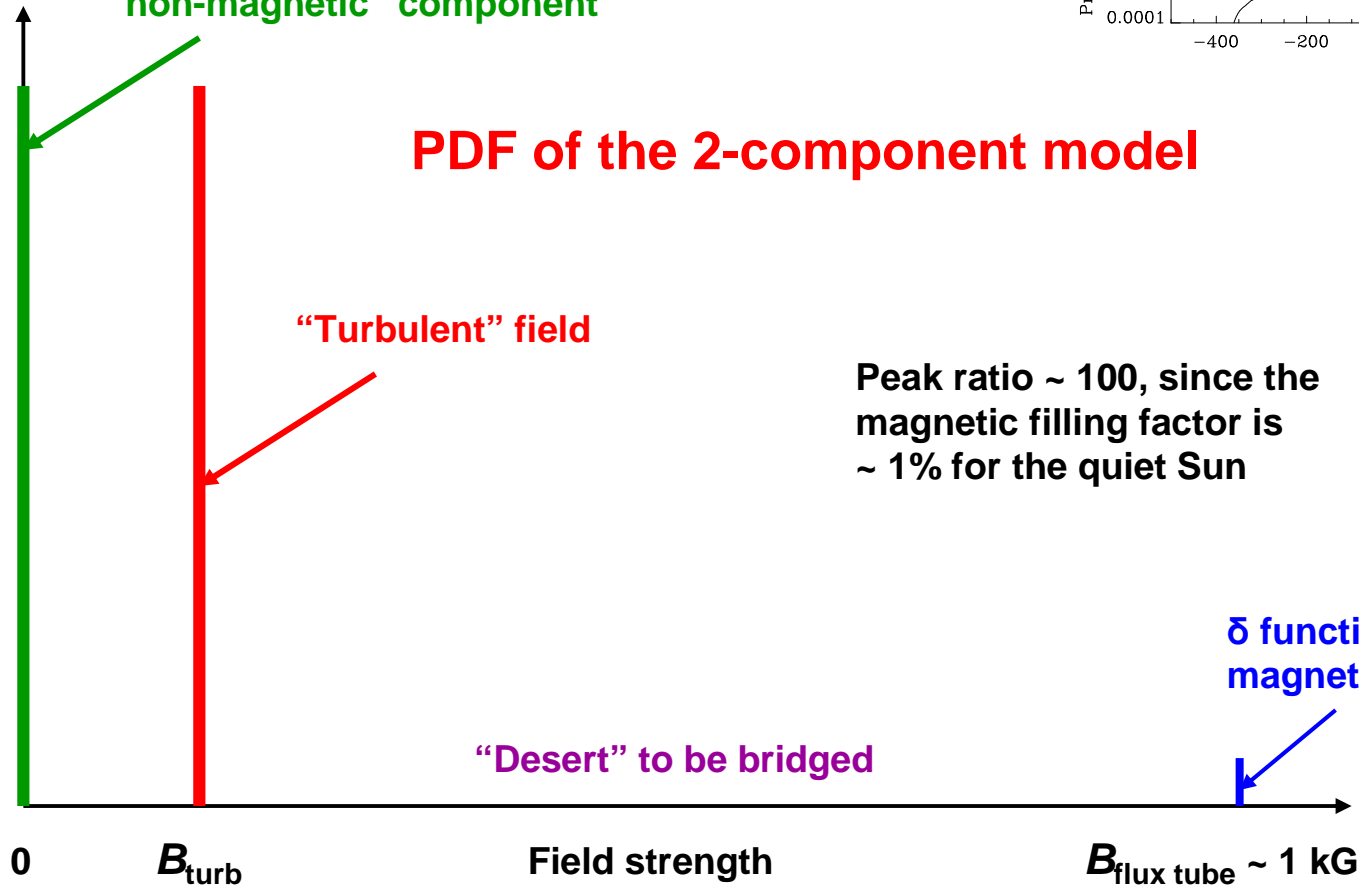
### PDF of the 2-component model

"Turbulent" field

Peak ratio ~ 100, since the magnetic filling factor is ~ 1% for the quiet Sun

$\delta$  function peak for magnetic component

"Desert" to be bridged



**Hinode, quiet Sun, spatial resolution ~ 200 km.**  
**The magnetic field is however structured on much smaller scales.**

1240

LITES ET AL.

Vol. 672

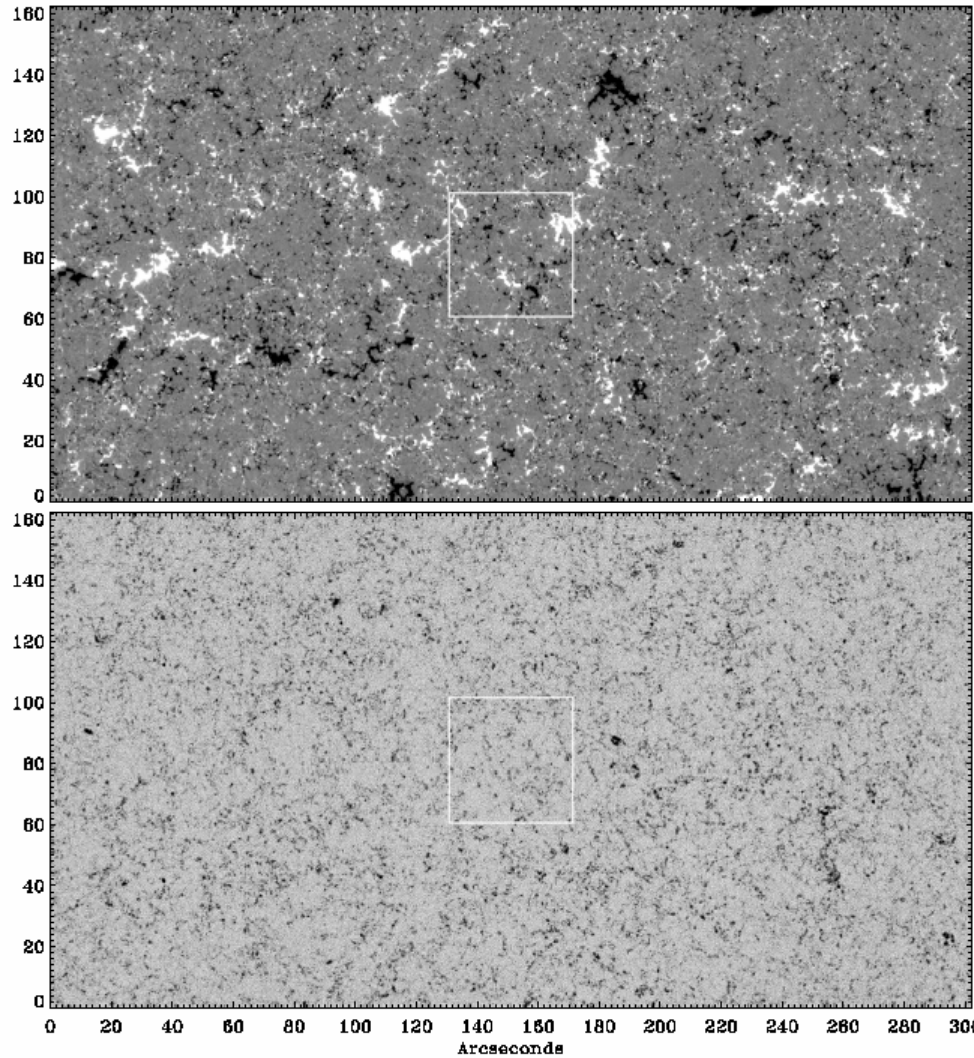


FIG. 2.—Vertical and horizontal apparent flux densities  $B_{app}^L$  (top) and  $B_{app}^T$  (bottom) for the quiet-Sun map of Fig. 1. The gray scale for  $B_{app}^L$  saturates at  $\pm 50 \text{ Mx cm}^{-2}$ , but it saturates at  $200 \text{ Mx cm}^{-2}$  for  $B_{app}^T$ . The highlighted central area is shown in Fig. 7, where the distinction between noise and real signal is more apparent.

IAU JD10, Rio de Janeiro, 10 August 2009

J.O. Stenflo

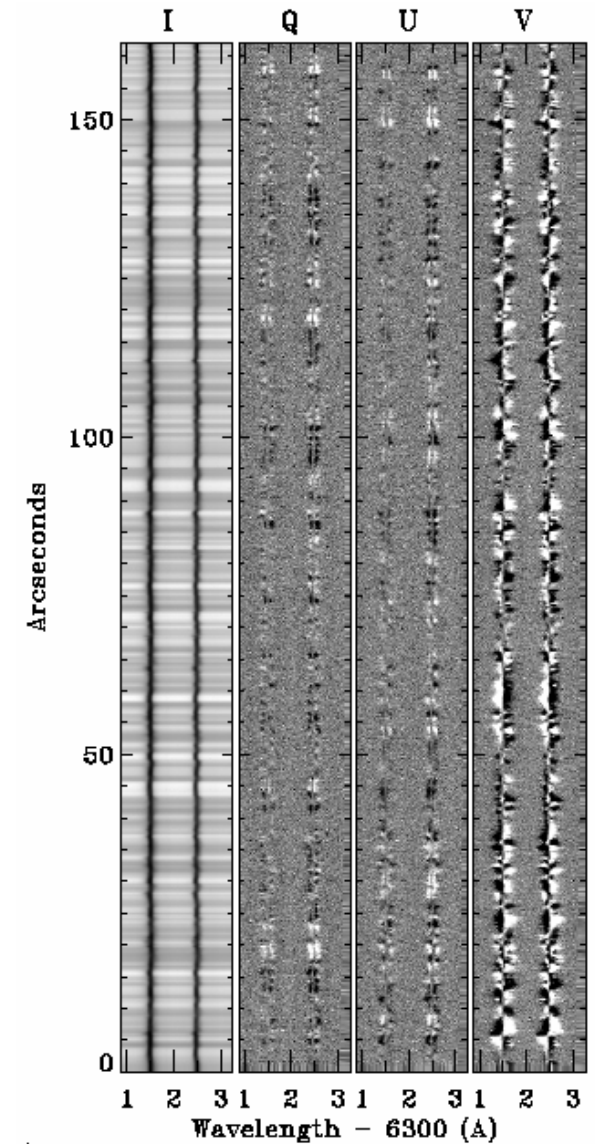
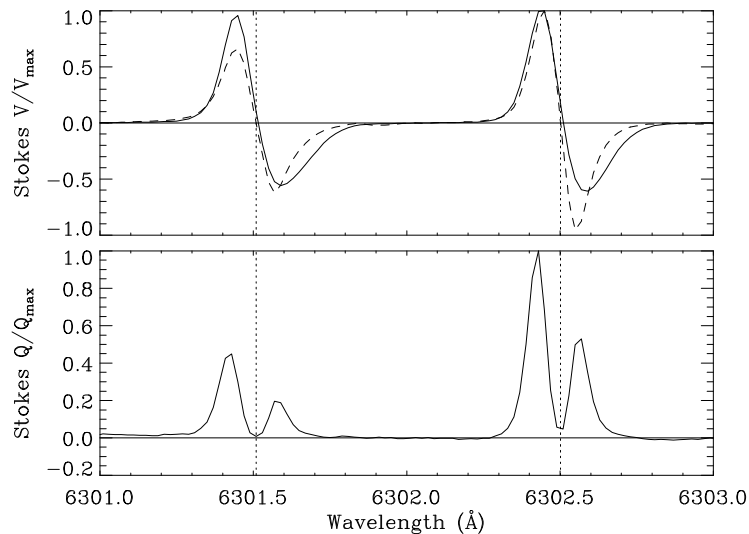


FIG. 10.—Typical deep mode, time-averaged Stokes  $I, Q, U, V$  spectrum from the observations presented in Fig. 11. These spectra were obtained at disk center with an integration time of 9.6 s. Guiding was programmed to track solar rotation. The time sequence of observations at a single slit position was subjected to a temporal running mean of seven observations, resulting in an effective integration time of 67.2 s. The noise level in the polarization continuum is about  $2.9 \times 10^{-4} I_c$ . The gray scale for  $Q, U, V$  saturates at  $\pm 0.001 I_c$ .



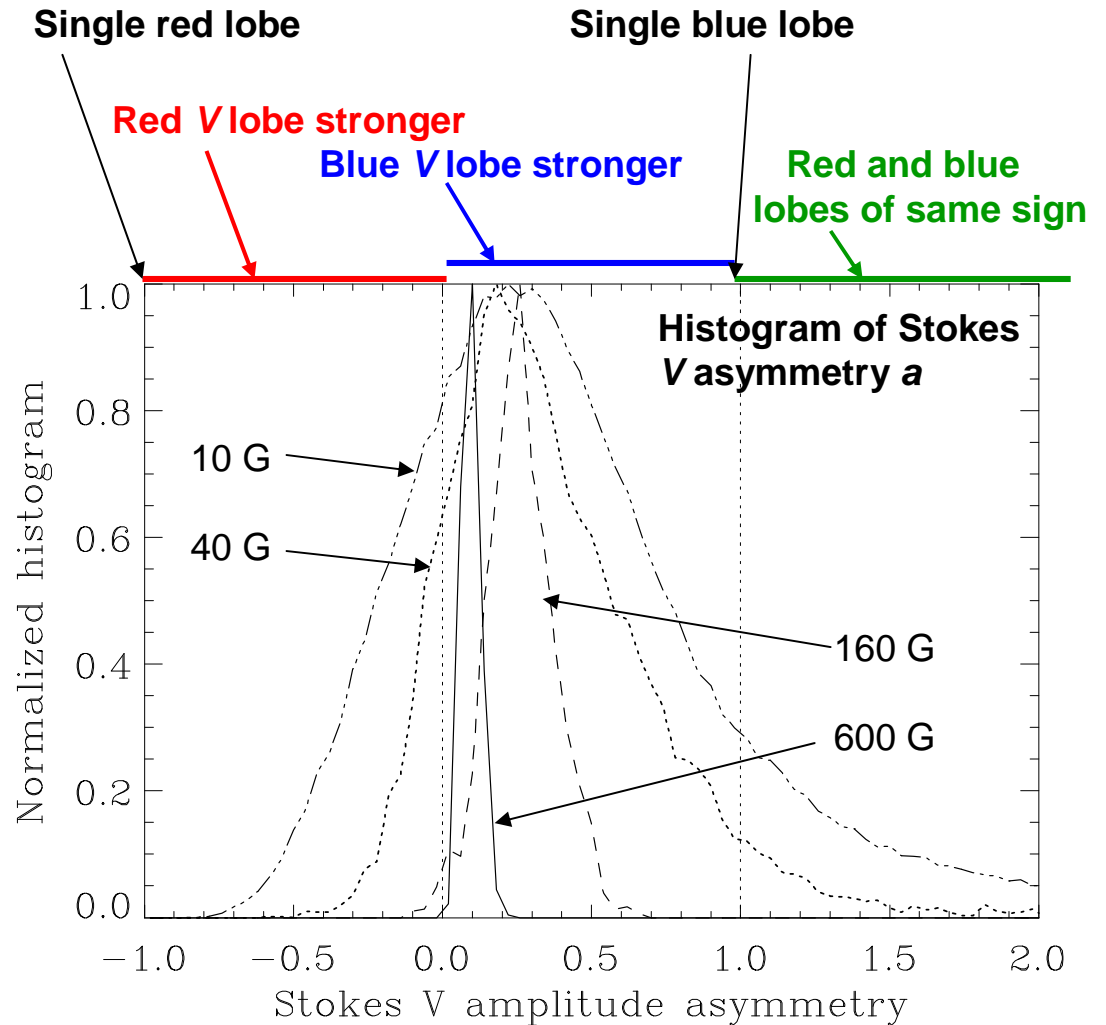
## Average Stokes V and Q profiles (Hinode quiet Sun)

Dashed curves:  $\partial I / \partial \lambda$



## Evidence from the Stokes V asymmetry $a$ of subresolution structuring

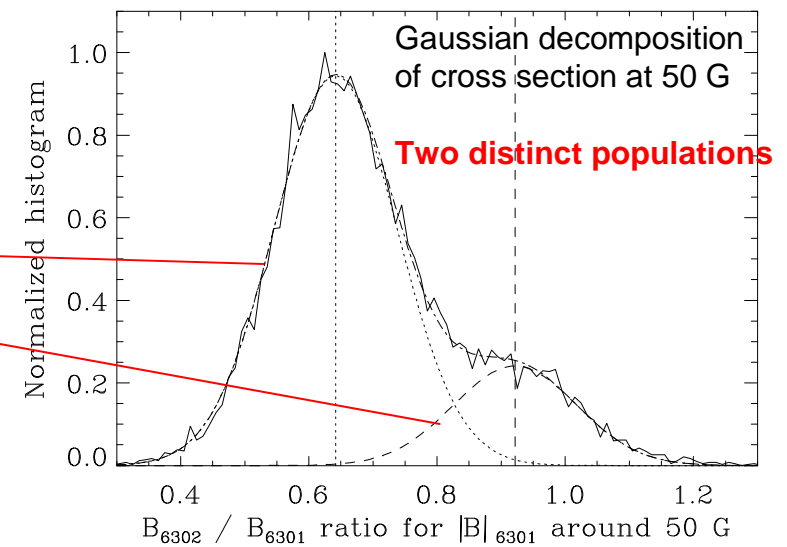
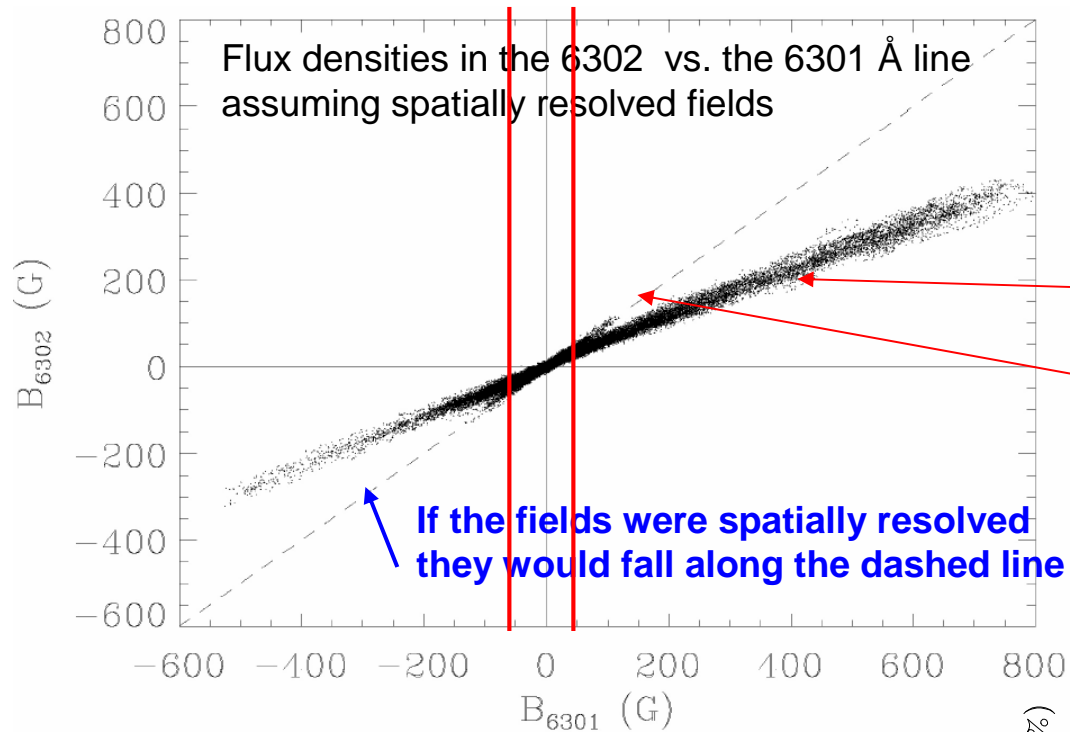
$$a = (V_{\text{blue}} + V_{\text{red}}) / (V_{\text{blue}} - V_{\text{red}})$$



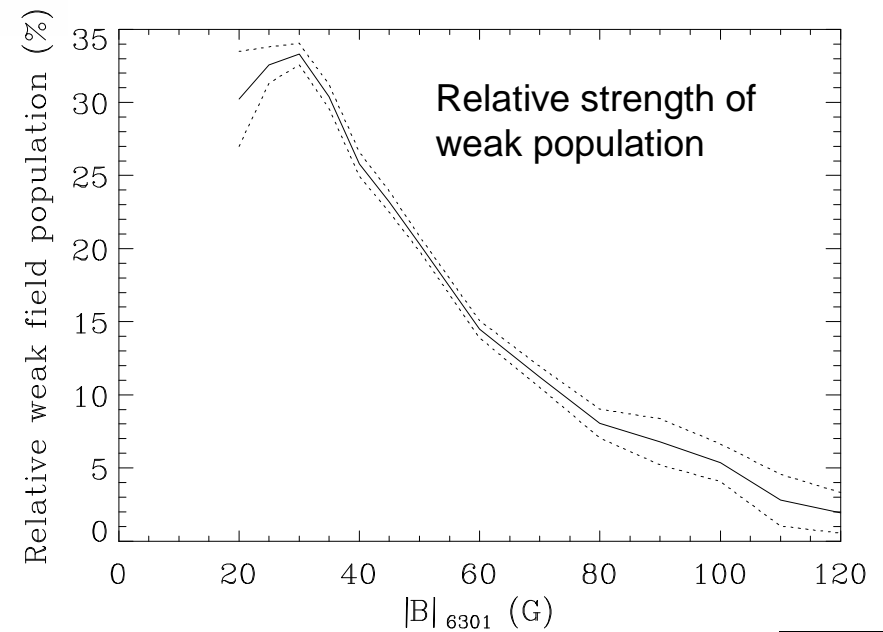
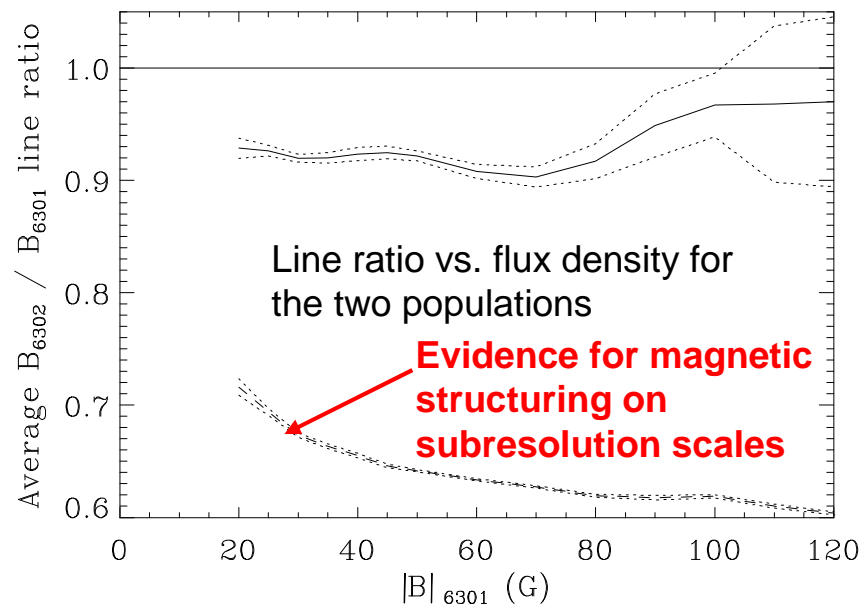
The asymmetry is due to subresolution correlations between spatial gradients of the magnetic and velocity fields.

There is an enormous spread in the V asymmetry for weak flux densities.

This is evidence for ubiquitous magnetic structuring at scales very much smaller than the Hinode 200 km resolution scale.



### Evidence from Stokes V line ratio

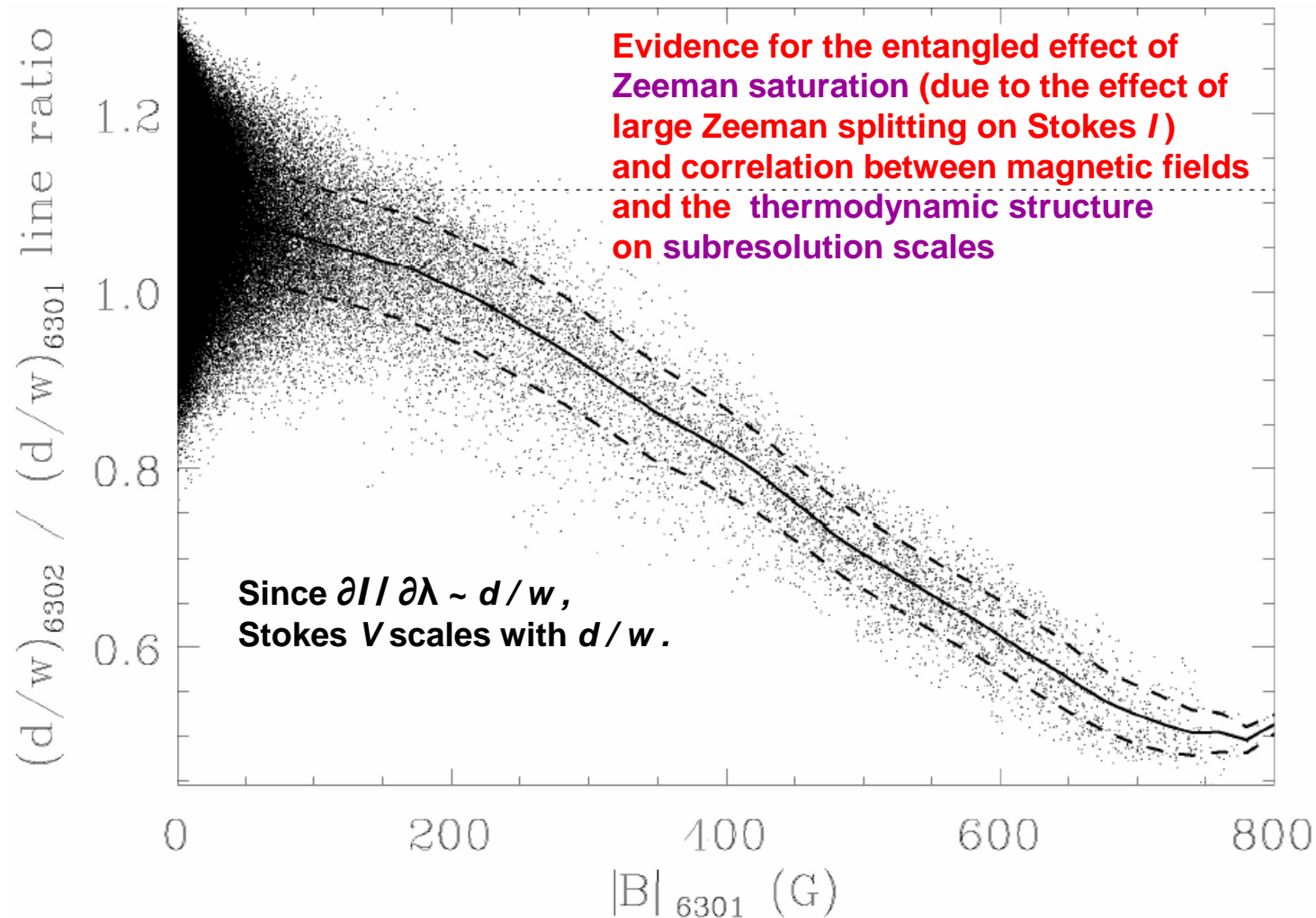


## Evidence from Stokes I – magnetic field correlations

Tight correlation between Stokes I (the intensity profile) and the magnetic flux density

6302 / 6301 line ratio in  $d/w$

$d$  = Stokes I line depth  
 $w$  = Stokes I line width

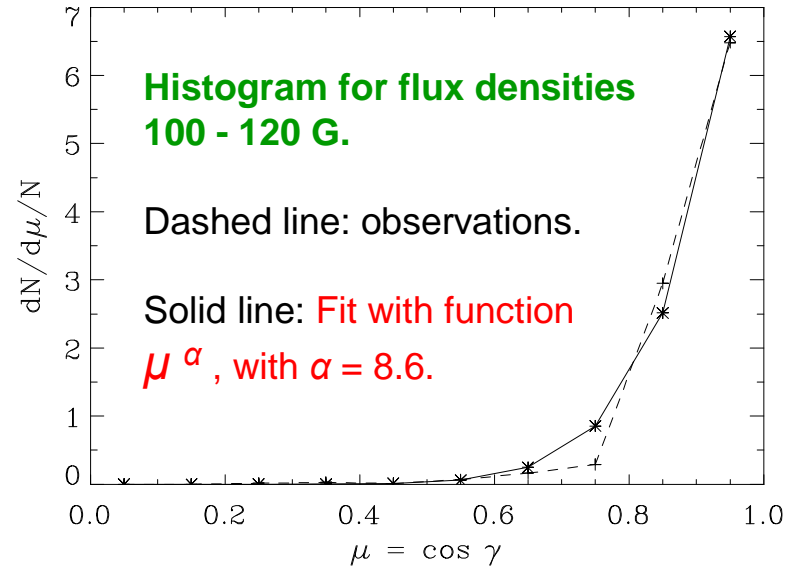
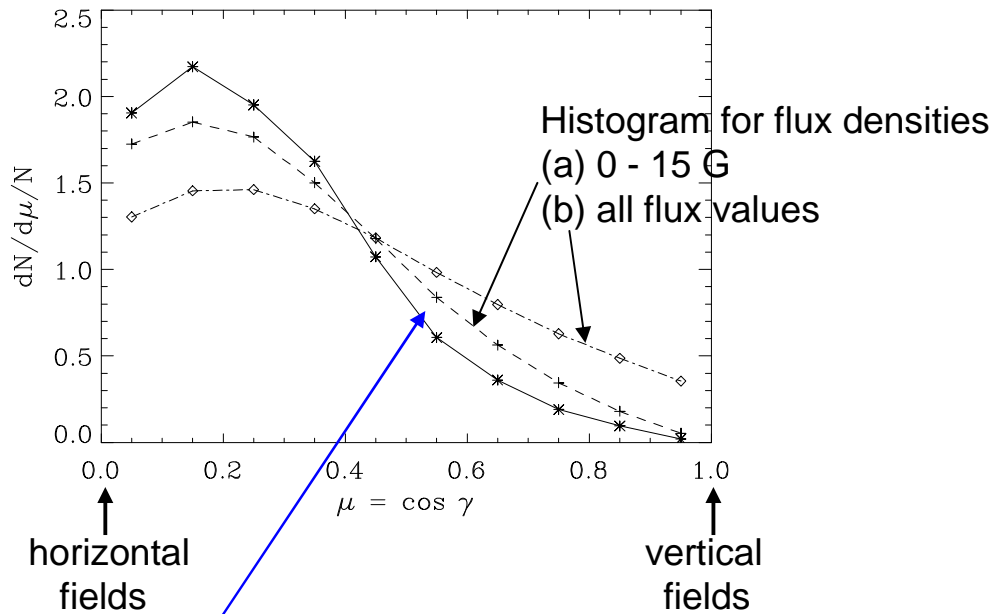


# Distributions of the inclination angle $\gamma$ of the magnetic field

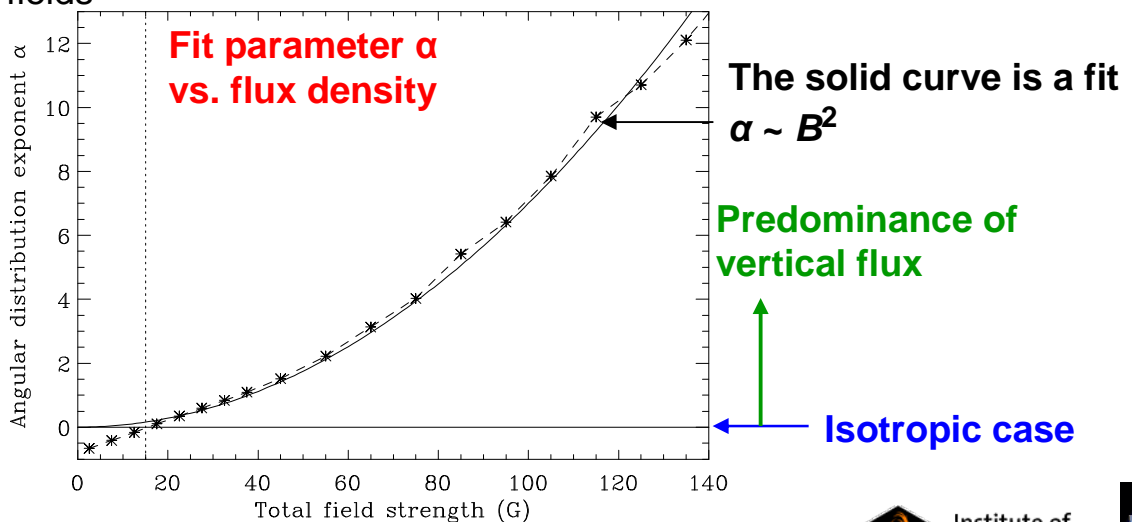
Horizontal PDF means isotropic distribution.

Negative slope means predominance of horizontal fields.

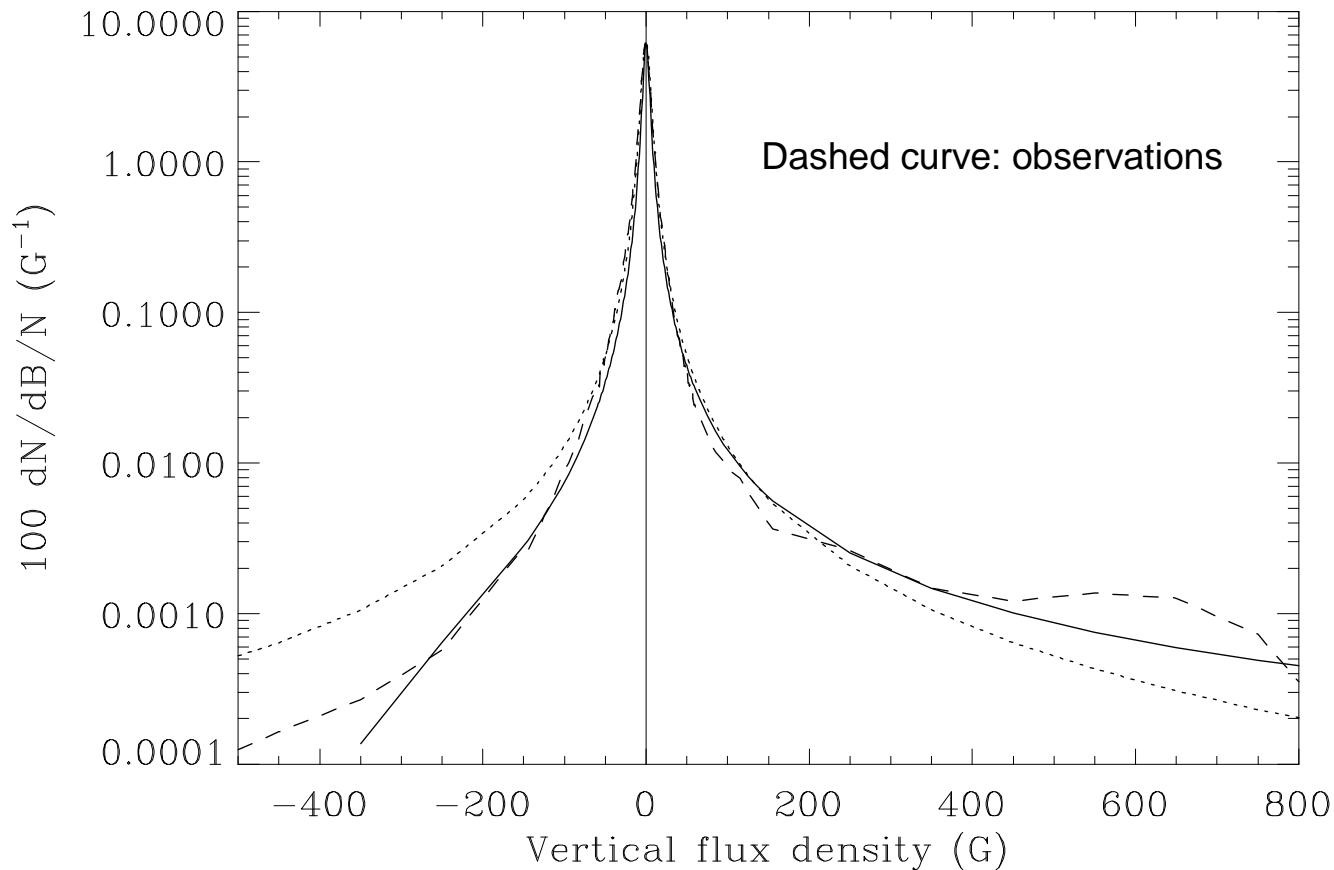
Positive slope means predominance of vertical fields.



Histogram exclusively due to the actual noise in the data, derived via Monte-Carlo simulation



## Probability density function for the vertical flux density



**Solid curve: representation of the noise-deconvolved observed histogram with a function that is the sum of a symmetric Lorentz profile and an anti-symmetric line dispersion profile.**

$$\left[ \left( \frac{\gamma}{2} \right)^2 + 0.038 B \right] / \left[ B^2 + \left( \frac{\gamma}{2} \right)^2 \right] \quad \gamma = 8 \text{ G}$$

**Dotted curve: the symmetric part (Lorentz function part) of this expression.**

# Estimate of the lower end of the scale spectrum

## Magnetic Reynolds number

$$R_m = \mu_0 \sigma \ell_c v_c$$

## Spitzer conductivity

$$\sigma = 10^{-3} T^{3/2} \text{ (SI units)}$$

## Kolmogorov turbulence (inertial range)

$$v_c = k \ell_c^{1/3} \text{ (where } k \text{ is a constant)}$$

With  $R_m = 1$  at the diffusion limit, and  $k = 25$   
(corresponding to 2.5 km/s for  $\ell_c = 1000$  km), we get

$$\ell_{\text{diff}} = 1 / (\mu_0 \sigma k)^{3/4}, \text{ or}$$

$$\ell_{\text{diff}} = 5 \times 10^5 / T^{9/8}$$

For  $T = 10,000$  K we get

$$\ell_{\text{diff}} = 15 \text{ m}$$



## Future steps

The magnetic structuring continues four orders of magnitude below the current spatial resolution limit.

For the spatially unresolved domain we need to transcend the 2-component approach to distribution functions (PDFs).

From the excellent Hinode data set for the quiet Sun we have inferred magnetic distribution functions for the strength and orientation of the field vector, valid for flux densities at the 200 km scale.

To infer the magnetic PDFs in the unresolved domain we first need to explore the **scaling laws** in the resolved domain and compare them with numerical simulations of magneto-convection.

The PDFs in the resolved domain appear to have a high degree of **scale invariance**, but this needs to be quantified in detail.



# Thank you !

